STRONG-STRONG SIMULATIONS OF COHERENT BEAM-BEAM EFFECTS IN THE EIC*

J. Qiang†, LBNL, Berkeley, California , U.S.A.

Y. Luo, C. Montag, D. Xu, F. Willeke, BNL, Long Island, New York, U.S.A.

Y. Hao, MSU, East Lansing, Michigan, U.S.A.

Abstract

The high luminosity electron ion collider (EIC) will provide great opportunities in nuclear physics study and is under active design. The coherent effects due to the beam-beam interaction of two colliding beams can cause beam size blow-up and degrade the luminosity in the EIC. In this paper, we report on the study of coherent beam-beam effects in the EIC design using self-consistent strong-strong simulations. These simulations show the coherent dipole and quadrupole mode instabilities in the tune working point scan and bunch intensity scan.

INTRODUCTION

The electron-ion collider (EIC) as a gluon microscope has been approved by the Department of Energy as the next major scientific facility that probes the detailed physics inside the nucleus with deep inelastic scattering using polarized high energy electron [1]. The EIC consists of two colliding rings, a hadron ring of 41-275 GeV and an electron storage ring of 5-18 GeV. The nominal design goal is to attain a peak luminosity of $\sim 10^{34}$/cm^2/s. The coherent instability driven by beam-beam interactions could cause beam size blow-up and degrade the peak luminosity [2-5]. Such an instability depends on the choice of transverse tune working points and beam bunch intensities as seen in the following strong-strong simulations.

COMPUTATION TOOL

The computational tool used in this study is a self-consistent strong-strong beam-beam code, BeamBeam3D [6,7]. The BeamBeam3D is a parallel three-dimensional particle-in-cell code to model beam-beam effects in high-energy ring colliders. This code includes a self-consistent calculation of the electromagnetic forces (beam-beam forces) from two colliding beams (i.e. strong-strong modeling), a linear and nonlinear high-order transfer map model for beam transport between collision points, a stochastic map to treat radiation damping, quantum excitation, a single map to account for chromaticity effects, a feedback model, an impedance model, and a Bremsstrahlung model. Here, the beam-beam forces can be from head-on collision, offset collision, and crossing angle collision. These forces are calculated by solving the Poisson equation using a shifted integrated Green function method, which can be computed very efficiently using an FFT-based algorithm on a uniform grid. For the crossing

angle collision, the particles are transformed from the lab frame into a boosted Lorentz frame following the procedure described by Hirata [8] and by Leunissen et al. [9], where the beam-beam forces are calculated in the same way as the head-on collision. After the collision the particles are transformed back into the laboratory frame. The BeamBeam3D code can handle multiple bunches from each beam collision at multiple interaction points (IPs). The parallel implementation is done using a particle-field decomposition method to achieve a good load balance.

SIMULATION RESULTS

The nominal design parameters used in the simulations are given in the following table. These design parameters

Table 1: EIC Design Parameters

	electron	proton
Energy (GeV)	10	275
Tune	(0.08,0.06)	(0.228,0.21)
Particles (10^{11})	1.72	0.69
Emittance (nm)	(20,1.1)	(11.3,1.0)
β^* (cm)	(55,5.6)	(80,7.2)
Beam-beam para.	(0.088,0.1)	(0.01,0.012)
Chromaticity	(1,1)	(1,1)
Damp time (k turn)	(4,4,2)	
Crab freq. (MHz)	394	197

were chosen to produce $\sim 10^{34}$/cm^2/s peak luminosity for the collision of a 10 GeV electron bunch and a 275 GeV proton bunch with 25 mrad crossing angle [10]. Pairs of crab cavities are used on both sides of the collision point to correct the crossing angle for both colliding beams. The nominal beam-beam parameters for the electron beam are (0.088, 0.1), and (0.01, 0.012) for the proton beam. The large beam-beam parameters result in strong coherent beam-beam effects. Such effects can cause instability due to the collective dynamic interactions between the electron beam and the proton beam.

In the EIC design, the transverse tune working points have to be carefully selected. Figure 1 shows the proton beam and electron beam horizontal centroid evolution with different choice of electron beam horizontal and vertical tunes. In this scan, the proton beam tune working point is fixed. It is seen that for the electron horizontal tune between 0.1 and 0.14, both electron and proton beam centroid become unstable.

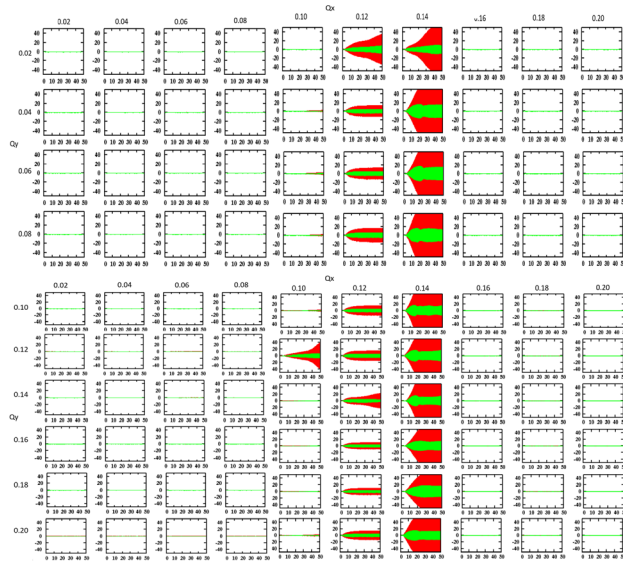To study the mechanism underlying these instabilities, we selected one electron tune working point (0.1,0.1).

Figure 1: Proton beam (red) and electron beam (green) horizontal centroid evolution with electron beam horizontal tune (Qx) and vertical tune (Qy) scan.

Figure 2 shows spectra of electron beam horizontal centroid evolution during three time windows: first 4000 turns, after 2000 turns, another 3000 turns. It is seen that spectrum amplitude of a single mode around 0.24 grows through three windows while the other mode amplitudes stay about the same. This suggests that this single becomes unstable and results in beam centroid blow-up.
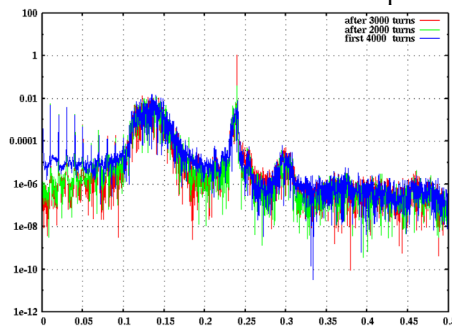

Figure 2: Spectra of electron centroid evolution during three periods of evolution.

Figure 3 shows the electron beam and proton beam horizontal centroid spectra with six electron horizontal tunes and one fixed vertical tune. It is seen that as the electron horizontal tune changes, the coherent electron mode frequency moves, while the coherent mode frequency from the proton beam stays the same. The electron beam becomes unstable only for the horizontal tunes between 0.1 and 0.14. This suggests a coupling resonance between the coherent electron mode and the coherent proton mode.

The above coherent dipole mode instability can be avoided by moving the proton beam working point. Figure 4 shows the proton beam and electron beam horizontal centroid evolution with two proton beam horizontal tunes.
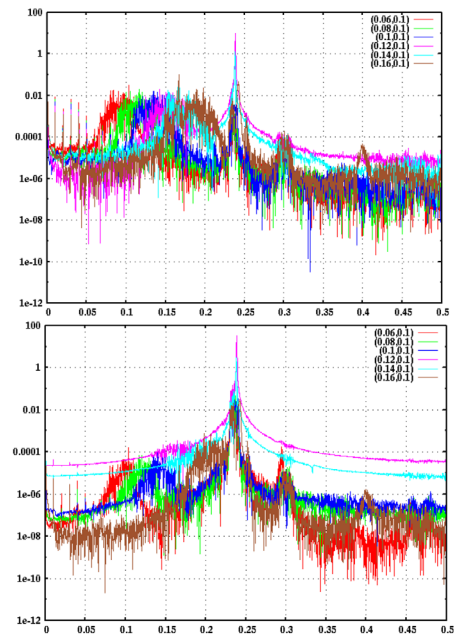

Figure 3: Electron (top) and proton (bottom) beam horizontal centroid spectra with different electron horizontal tunes.

It is seen that by moving the proton beam tune away from the resonance, both beams become stable.
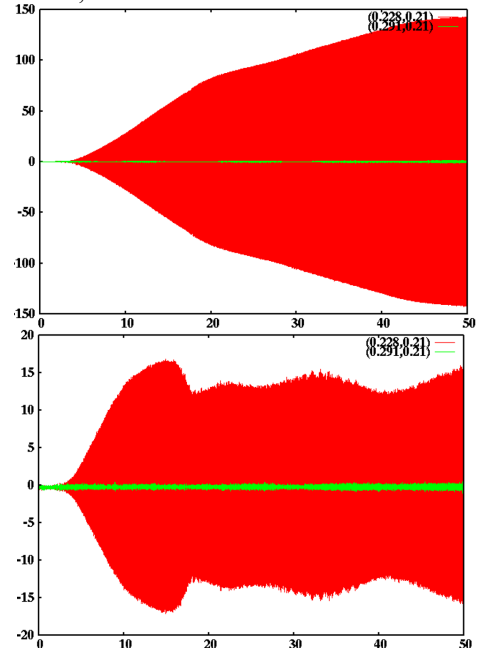

Figure 4: Proton beam (top) and electron beam (bottom) horizontal centroid evolution with two proton beam horizontal tunes.

Besides scanning the electron beam transverse working points, we also scanned the proton beam transverse tunes. Figure 5 shows the peak luminosity as a function of proton beam horizontal and vertical tunes. It is seen that the good luminosity stays below the diagonal line of the tune space. Near the diagonal line, coherent coupling resonance occurs and causes the degradation of luminosity.
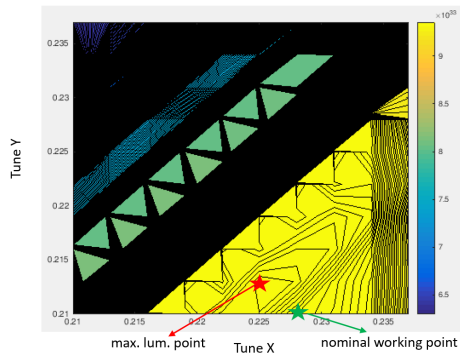
Figure 5: Peak luminosity as a function of proton beam horizontal and vertical tunes.

Coherent instability also occurs during the beam intensity scan. Figure 6 shows electron beam and proton beam RMS size evolution with several proton beam intensities. Here, 1 means the nominal proton beam intensity, 0.8 means 0.8 times the nominal intensity. It is seen that when the proton beam lowers to 0.4 times the nominal proton intensity, both the electron beam and the proton beam become unstable.
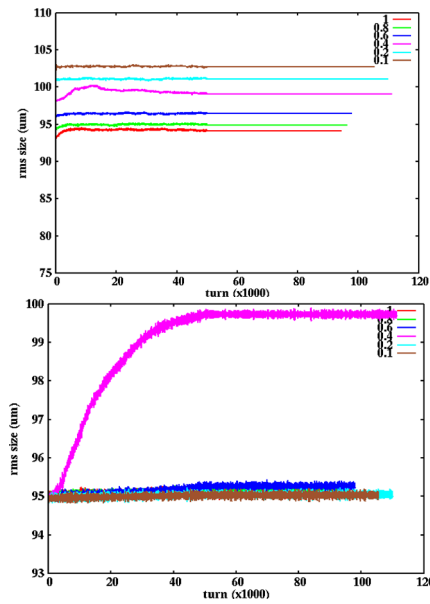

Figure 6: Electron beam (top) and proton beam (bottom) horizontal RMS size evolutions with several proton beam bunch intensities.

To understand the mechanism of this instability, we calculated the tune footprints of the electron beam in Figure 7. It is seen that as the proton beam intensity decreases, the beam-beam forces become weaker, and the electron beam tune footprint become smaller. There is no particular lower order resonance for the x0.4 proton intensity. This suggests that instability should not be a dipole mode instability.

Figure 8 shows the spectra of electron and proton beam horizontal RMS size evolution through these proton beam intensity scan. It appears that for x0.4 proton intensity the electron beam quadrupole mode hits the 5th order resonance with too small tune spread to stabilize the beam. Further lower the proton intensity moves away from the resonance,
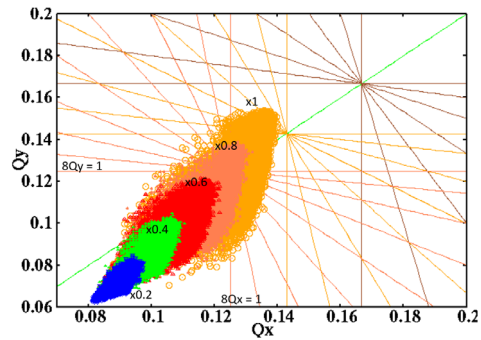

Figure 7: Electron beam tune footprint with several proton beam bunch intensities.

while further increase the proton intensity results in a larger tune spread and stabilize the instability through the Landau damping.
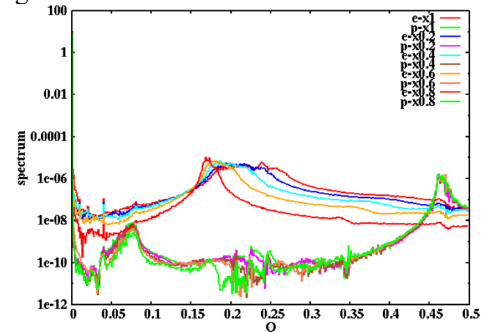

Figure 8: Spectra of electron beam and proton beam horizontal RMS size evolution with several proton beam bunch intensities.

We also scanned electron beam intensity as shown in Fig. 9. It is seen that proton beam emittance growth rate increases quickly after the electron intensity attains 3.5 x10^{11}. This is due to the large proton beam-beam parameter (~0.019) across the 4th order coherent resonance and results in large emittance growth.

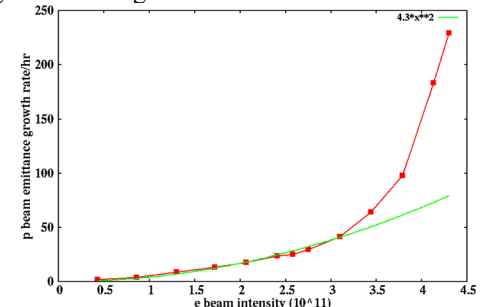Figure 9: Proton beam emittance growth rate as a function electron beam bunch intensity.

SUMMARY

In this study, using the self-consistent strong-strong beam-beam simulations, we observed coherent instabilities of both dipole and quadrupole modes in the transverse tune working point scan and the beam intensity scan. These instabilities can be avoided by appropriately choosing working points and beam intensity parameters.

REFERENCES

[1] J. Beebe-Wang *et al.*, "Electron-Ion-Collider at Brookhaven National Laboratory Conceptual Design Report," 2021. doi:10.2172/1765663

[2] A. W. Chao and R. D. Ruth, "Coherent beam-beam instability in colliding-beam storage rings", *Particle Accelerators*, vol. 16, p. 201, 1985.

[3] Y. Hao and V. Ptitsyn, "Effect of electron disruption in the energy recovery linac based electron ion collider", *Phys. Rev. ST Accel. Beams,* vol. 13, p. 071003, 2010. doi:10.1103/PhysRevSTAB.13.071003

[4] S. White, X. Buffat, N. Mounet, and T. Pieloni, "Transverse mode coupling instability of colliding beams", *Phys. Rev. Accel. Beams*, vol. 17, p. 041002, 2014. doi:10.1103/PhysRevSTAB.17.041002

[5] K. Ohmi, N. Kuroo, K. Oide, D. Zhou, and F. Zimmermann, "Coherent Beam-Beam Instability in Collisions with a Large Crossing Angle", *Phys. Rev. Lett.*, vol. 119, p. 134801, 2017. doi:10.1103/PhysRevLett.119.134801

[6] J. Qiang, M. A. Furman, R. D. Ryne, "A Parallel Particle-in-Cell Model for Beam-Beam Interaction in High Energy Ring Colliders", *J. Comp. Phys.*, vol. 198, p. 278, 2004. doi:10.1016/j.jcp.2004.01.008

[7] J. Qiang, M. Furman, and R. Ryne, "Strong-strong beam-beam simulation using a Green function approach", *Phys. Rev. ST Accel. Beams*, vol. 5, p. 104402, 2002. doi:10.1103/PhysRevSTAB.5.104402

[8] K. Hirata, "Analysis of Beam-Beam Interactions with a Large Crossing Angle", *Phys. Rev. Lett.*, vol. 74, no. 12, p. 2228, 1995.

[9] L.H.A. Leunissen, F. Schmidt, G. Ripken, "Six-dimensional beam-beam kick including coupled motion", *Phys. Rev. ST Accel. Beams*, vol. 3, p. 124002, 2000. doi:10.1103/PhysRevSTAB.3.124002

[10] Y. Luo *et al.*, "Beam-Beam Related Design Parameter Optimization for the Electron-Ion Collider", in *Proc. IPAC'21*, Campinas, Brazil, May 2021, pp. 3808-3811. doi:10.18429/JACoW-IPAC2021-THPAB028